Colloids and Surfaces B: Biointerfaces 66 (2008) 266–273

Contents lists available at ScienceDirect

Colloids and Surfaces B: Biointerfaces

journal homepage: www.elsevier.com/locate/colsurfb

Amperometric determination of H_2O_2 at nano-TiO_2/DNA/thionin nanocomposite modified electrode

Po-Hsun Lo, S. Ashok Kumar, Shen-Ming Chen*

Department of Chemical Engineering and Biotechnology, National Taipei University of Technology, No. 1, Section 3, Chung-Hsiao East Road, Taipei, 106, Taiwan, ROC

ARTICLE INFO

Article history:
Received 4 May 2008
Received in revised form 10 June 2008
Accepted 2 July 2008
Available online 12 July 2008

Keywords:
DNA modified electrode
Hydrogen peroxide detection
Nanostructured TiO_2
Electrocatalysis
Biosensors

ABSTRACT

We report electrochemical preparation and characterization of a new biosensor made of nanostructured titanium dioxide (nano-TiO_2) particles and deoxyribonucleic acid (DNA). Thionin (TN) redox mediator was electrochemically deposited onto DNA/nano-TiO_2 modified glassy carbon electrode (GCE). The X-ray diffraction analysis, atomic force microscope (AFM) and scanning electron microscope (SEM) were used for surface analysis of TN/DNA/nano-TiO_2 film. In neutral buffer solution, TN/DNA/nano-TiO_2/GCE biosensor exhibited excellent electrocatalytic activity towards the reduction of hydrogen peroxide (H_2O_2) and oxygen (O_2). The biosensor shows excellent analytical performance for amperometric determination of H_2O_2, at reduced overpotential (−0.2 V). The detection limit and liner calibration range were found to be 0.05 mM (S/N = 3) and 0.05–22.3 mM, respectively. In addition, determination of H_2O_2 in real samples was carried out using the new biosensor with satisfactory results. The TN/DNA/nano-TiO_2/GCE showed stable and reproducible analytical performance towards the reduction of H_2O_2. This biosensor can be used as an amperometric biosensor for the determination of H_2O_2 in real samples.

1. Introduction

Metal oxides are emerging as important materials because of their versatile properties such as high-temperature superconductivity, ferroelectricity, ferromagnetism, piezoelectricity and semiconductivity. Recently, nanostructured TiO_2 particles preparation and their applications in photovoltaic studies, photocatalysis and environmental studies (water and air purification) have attracted much attention among the researchers [1–6]. The emerging sensor technology based on nanoparticles (NPs) and nanocomposites with chemical and biological molecules is much beneficial for direct and real applications. For example, the TiO_2–oligonucleotide nanocomposites not only retain the intrinsic photocatalytic capacity of TiO_2 and the bioactivity of the oligonucleotide DNA, but also possess the chemically and biologically unique new property of a light-inducible nucleic acid endonuclease, which could became a new tool for gene therapy [7]. Recent advances in hybrid nanotechnology involving nucleic acids are predominantly linked with sequence-specific nucleic acid interactions, and are oriented towards cellular imaging or DNA microarray development [8–11].

Recently, the anti-17β-estradiol antibody was immobilized on polyelectrolyte polyacrylic acid-modified TiO_2 nanoparticles for water treatment [12], sonogel carbon electrode modified with nanostructured TiO_2 for catechol detection [13], a nano-TiO_2 film/nafion modified on a glassy carbon electrode (GCE) used for investigation of dopamine [14], nano-TiO_2 and hemoglobin were co-modified on pyrolytic graphite electrode to study the photovoltaic effect of TiO_2 nanoparticles [15,16] and carbon electrode modified with TiO_2/metal nanoparticles for the detection of trinitrotoluene [17] have been reported.

The DNA has been used for the immobilization of protein molecules [18–22]. DNA can enhance electron transfer between electrode and heme proteins in myoglobin–DNA films [23]. Hemoglobin on DNA/poly-2,6-pyridinediamine modified Au electrode for detection of H_2O_2 [24], DNA/poly(*p*-aminobenzensulfonic acid) bi-layer modified GCE for detection of dopamine and uric acid [25], electrochemical behavior of neomycin at DNA-modified gold electrodes are investigated [26]. An electrochemically deposited thin film of DNA is suitable platform for fabrication of biosensors [27–29].

In the present work, we report a novel nanocomposite biosensor for the detection of H_2O_2 based on thionin incorporated bi-layer of DNA/nano-TiO_2 film modified electrode. X-ray diffraction pattern, atomic force microscope (AFM) and scanning electron microscope (SEM) have been employed for surface characterizations of TN/DNA/nano-TiO_2 films modified electrode. Cyclic

* Corresponding author. Tel.: +886 2 27017147; fax: +886 2 27025238.
E-mail addresses: sakumar80@gmail.com (S.A. Kumar), smchen78@ms15.hinet.net (S.-M. Chen).

0927-7765/$ – see front matter © 2008 Elsevier B.V. All rights reserved.
doi:10.1016/j.colsurfb.2008.07.003

voltammetry and amperometry have been used for investigation of electrochemical properties of nanocomposite modified electrode. Using amperometry, linear range and detection limit of H_2O_2 were explored. In addition, we report electrocatalytic reduction of oxygen (O_2) using TN/DNA/nano-TiO_2 coated electrode.

2. Experimental

2.1. Materials and apparatus

Deoxyribonucleic acid sodium salt (17.5 A_{260} units/mg), thionin dye (dye content >95%) and titanium oxosulfate $TiOSO_4$ were purchased from Sigma–Aldrich (St. Louis, MO, USA). H_2O_2 (30%, w/w), potassium ferrocyanide, sulfuric acid (H_2SO_4, assay 95%), nitric acid (HNO_3, assay 60%) and sodium hydroxide (purity 93%) were purchased from Wako pure chemicals (Osaka, Japan). Potassium nitrate, sodium acetate and sodium dihydrogen phosphate were received from E-Merck (Darmstadt, Germany) and other chemicals were of analytical grade and used without further purification. Double-distilled water was used in all experiments. Diluted H_2O_2 standard solutions were freshly prepared directly prior to use. The commercial antiseptic and contact lenses cleaning H_2O_2 solutions were purchased from a local drug store in Taipei.

Electrochemical measurements were performed by a CHI750A Electrochemical Work Station (CH Instrument Inc., USA). Glassy carbon electrode from BAS (West Lafayette, USA) and indium tin oxide-coated glass (ITO) electrodes were purchased from Merck Display Technologies, Ltd. (Darmstadt, Germany). ITO thickness and resistance were 30 ± 10 nm and 80 Ω, respectively. Size of the glass: 300 mm × 350 mm × 0.7 mm. ITO or GCE are used as working electrodes. ITO substrates were cleaned by using detergent, diluted nitric acid and then finally rinsed with distilled water. Platinum wire is used as the counter electrode. All the cell potentials were measured with respect to an Ag/AgCl [KCl (sat)] reference electrode. Amperometry measurements for H_2O_2 were performed on a Bi-potentiostat Model CHI750A (TX, USA) having an analytical rotator model AFMSRK with MSRX speed control (PINE Instruments, USA). Hitachi scientific instruments (London, UK) model S-3000H scanning electron microscope was used for surface image measurements. The AFM images were recorded with a multimode scanning probe microscope system operated in tapping mode using Being Nano-Instruments CSPM-4000, Ben Yuan Ltd. (Beijing, China). Electrochemical impedance measurements were performed using impedance measurement unit, IM6ex ZAHNER, Messsysteme (Kroanch, Germany). All experiments were carried out at room temperature.

2.2. Electrochemical synthesis of TiO_2

Electrochemical synthesis of TiO_2 nanoparticles were carried out onto ITO electrode from the bath solution containing 0.02 M $TiOSO_4$, 0.03 M H_2O_2, 0.05 M HNO_3 and 0.05–0.25 M KNO_3 (pH 1.4). The deposition was performed at room temperature (25 ± 2 °C) under potentiostatic conditions (−2.0 V vs. Ag/AgCl). This led to the formation of a white colored gel film on the electrode surface. Each deposition has been conducted for 30 min. For the preparation of multiple TiO_2 layers electrosynthesis was repeated three or four times, with drying steps at 150 °C in between, after which the final annealing step takes place at 400 °C for 1 h to obtain crystalline TiO_2 film. The substrates were weighed prior to coating and after annealing to determine the amount of deposited TiO_2. Nearly 20% mass reduction was observed after heat-treatment at 400 °C for 1 h, due to water elimination from the film [30]. Thereafter, crystalline TiO_2 particles were scratched from the ITO surface and collected in 10 mL brown colored vial and later used for modification of GCE.

Cathodic electro-deposition of TiO_2 film from $TiOSO_4 + H_2O_2 + HNO_3 + KNO_3$ (pH 1.4) solutions involves the indirect deposition of a gel of hydrous titanium oxo-hydrides (Eq. (3)), resulting from the reaction of titanium peroxo-sulfate Eq. (2) with hydroxide ions produced by nitrate electrochemical reduction [30–32].

$$NO_3^- + H_2O + 2e^- \rightarrow NO_2^- + 2OH^- \quad (1)$$

$$TiOSO_4 + H_2O_2 \rightarrow Ti(O_2)SO_4 + H_2O \quad (2)$$

$$Ti(O_2)SO_4 + 2OH^- + (x+1)H_2O \rightarrow TiO(OH)_2{\cdot}xH_2O_2 + SO_4^{2-} \quad (3)$$

Annealing of the gel at 400 °C for an hour, results in the formation of crystalline TiO_2.

$$TiO(OH)_2{\cdot}xH_2O \rightarrow TiO_2 + (x+1)H_2O. \quad (4)$$

2.3. Preparation of modified electrodes

2.5 mg of synthesized TiO_2 NPs was added into 5 mL double-distilled water and then ultrasonicated for 10 min to create a suspension with a concentration of 0.5 mg mL^{-1}. After being diluted five times, the mixture of 10 μL TiO_2 NPs suspension was spread evenly onto the surface of the well cleaned GCE which was dried for 6 h in the absence of light. Finally, the modified electrode was thoroughly rinsed with double-distilled water. The deposition of DNA layer was carried out under constant potential of +1.5 V for 30 min in 0.1 mg mL^{-1} DNA solution [25,33]. This electrode was described as DNA/nano-TiO_2/GCE. For comparison, the DNA deposition was made on a bare GCE to prepare a DNA modified GCE, denoted as DNA/GCE.

Consequently, DNA/nano-TiO_2/GCE electrode was cycled in 0.1 M phosphate buffer solution (PBS) containing 1×10^{-5} M thionin (between −0.45 and 0.2 V) for 20 cycles. Afterwards, the electrode was thoroughly rinsed with double-distilled water and then dried at 4 °C for an hour in the absences of light. When not in use, the electrode was stored in aqueous solution of 0.1 M PBS (pH 7.0) at 4 °C. It was named as TN/DNA/nano-TiO_2/GCE and then used for further studies. For comparison, TN/nano-TiO_2/GCE, TN/DNA/GCE and TN/GCE coated electrodes were prepared and used for further investigation.

3. Results and discussions

3.1. Electrochemical deposition of TN

Fig. 1 shows the consecutive cyclic voltammograms (CVs) of TN adsorption onto DNA/nano-TiO_2 bi-layer modified electrode in pH 7.0 PBS containing 1×10^{-5} M TN. The CVs of the electrochemical deposition of TN film onto a DNA/nano-TiO_2/GCE was characterized by the TN redox couple in the scanning potential region between 0.0 and −0.4 V. The continuous increase in anodic and cathodic peak currents of the TN redox couple indicated the surface deposition of TN molecules (Fig. 1). After the 20th cycle, TN adsorption reached saturation. According to the literature reports, DNA is negatively charged [24–26] which could be firmly attached onto biocompatible nano-TiO_2 layer [7]. The irreversible doping of TN occurs onto DNA/nano-TiO_2 layer due to the interaction between negatively charged DNA and the positively charged TN from its solution (pK_a 7.8) [34]. In this experiment, during the electrochemical deposition process, TN

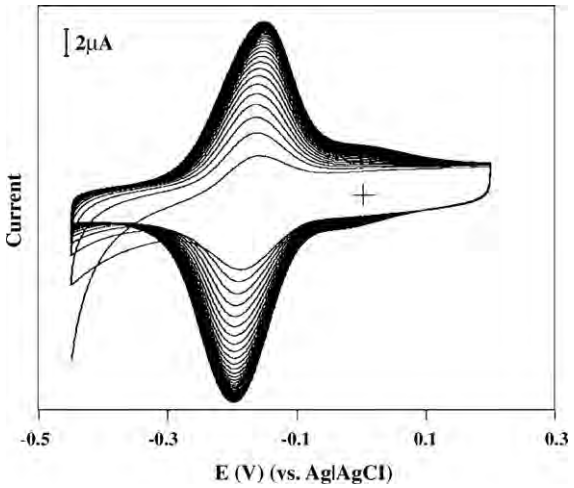

Fig. 1. CVs of TN monomers deposition onto DNA/nano-TiO_2 modified GCE from PBS (pH 7.0) containing 1×10^{-5} M TN.

monomers were adsorbed (not polymerized) onto DNA/nano-TiO_2 bi-layer.

3.2. Surface characterizations

Fig. 2 shows the SEM and AFM images of nano-TiO_2 (a and d), DNA/nano-TiO_2 (b and e) and TN/DNA/nano-TiO_2 (c and f) coated electrodes. From AFM image analyzer the size of the TiO_2 particles was found to be 40 ± 20 nm (a and d). Topography of DNA/nano-TiO_2 bi-layer films confirmed that nanocomposite evenly covered the electrode surface, as seen in Fig. 2(b and e). The TN/DNA/nano-TiO_2 film layer surface is highly porous and almost uniformly covered the electrode surface (c and f). The average surface roughnesses of nano-TiO_2, DNA/nano-TiO_2 and TN/DNA/nano-TiO_2 film electrodes are 1.6, 4.4 and 1.7 nm, respectively. Fig. 3 shows the X-ray diffraction images of TiO_2 particles. The experimental spacing were compared with those reported for rutile (1 1 0) (2θ of 27.45°) and anatase (1 0 1) (25.24°) to identify the particle structure [32]. XRD results revealed that synthesized particles are mainly composed of anatase.

Electrochemical impedance studies: A Nyquist diagram of electrochemical impedance spectrum is an effective way to measure the

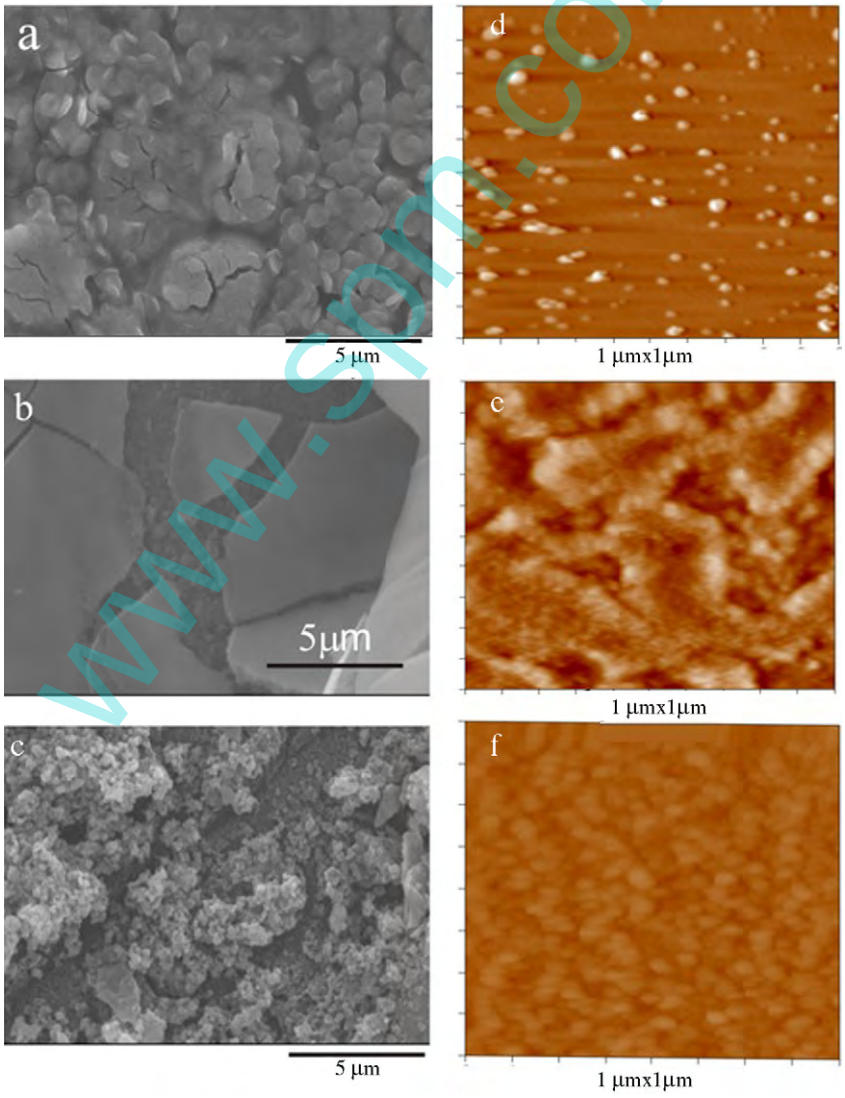

Fig. 2. SEM and AFM images of nano-TiO_2 (a and d), DNA/nano-TiO_2 (b and e) and TN/DNA/nano-TiO_2 (c and f) films.

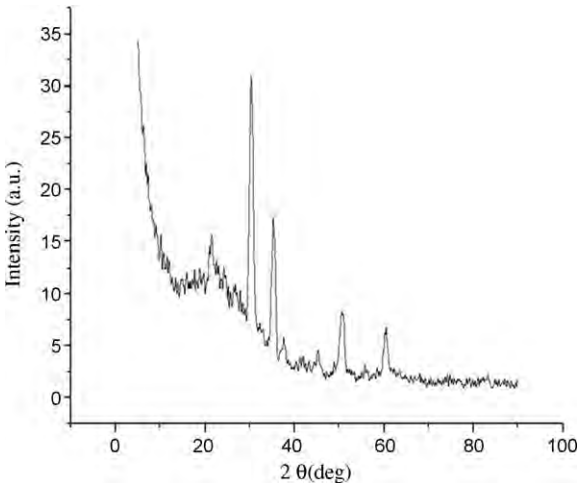

Fig. 3. X-ray diffraction image of nano-TiO_2 particles.

electron-transfer resistance. Fig. 4 shows Nyquist plots of bare GCE, nano-TiO_2/GCE, DNA/nano-TiO_2/GCE and TN/DNA/nano-TiO_2/GCE in the presence of 1 mM $[Fe(CN)_6]^{3-/4-}$ probe in pH 7.0 PBS. As shown in Fig. 4 each of the impedance spectra includes a semicircle part and a linear line part, corresponding to the electron-transfer process and the diffusion process, respectively. The diameter of the semicircle represents the electron-transfer resistance (R_{et}) at the electrode surface. As shown in Fig. 4, curve (a) is a Nyquist plot of a bare GCE in 1 mM $[Fe(CN)_6]^{3-/4-}$. A very small semicircle domain (R_{et} = 100 Ω) was found, which implied a very low electron-transfer resistance to the redox probe. After a modification with nano-TiO_2 layer, the electron-transfer resistance reached a higher value (curve b, R_{et} = 700 Ω). Further modification of DNA with nano-TiO_2 film modified electrode reached a higher value of electron-transfer resistance (curve c, R_{et} = 1410 Ω). Electron-transfer resistance (curve d, R_{et} = 810 Ω) of TN/DNA/nano-TiO_2/GCE decreased dramatically, which indicated that TN adsorption on bilayer facilitates the electron transfer of the electrochemical probe on the bilayer modified electrode. The increase of electron-transfer kinetics on the electrode surface originates from the TN monolayer. The high conductivity of TN/DNA/nano-TiO_2/GCE nanocomposite film increases the electrical properties of the redox processes and also provides a large surface area available for TN intercalation.

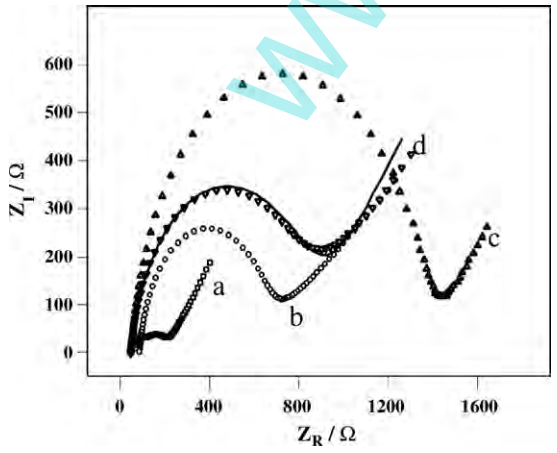

Fig. 4. Electrochemical impedance spectra of (a) bare GCE, (b) nano-TiO_2/GCE, (c) DNA/nano-TiO_2/GCE and (d) TN/DNA/nano-TiO_2/GCE in 1 mM $[Fe(CN)_6]^{3-/4-}$ + 0.1 M PBS.

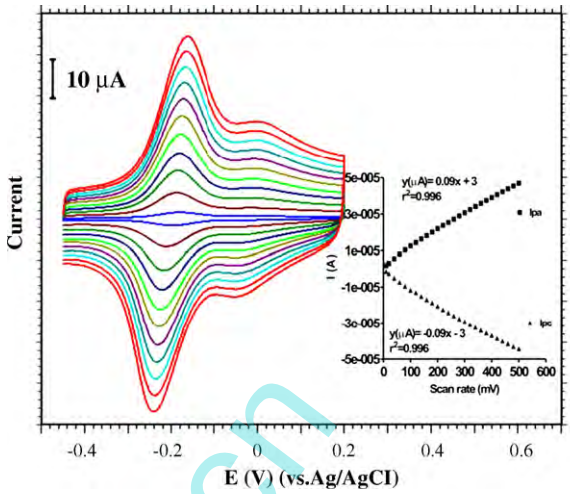

Fig. 5. CVs of TN/DNA/nano-TiO_2/GCE in pH 7.0 PBS at different scan rates, the scan rates from inner to outer are 0.01–0.50 V s^{-1}, respectively. Inset figure shows I_{pa} and I_{pc} vs. scan rate.

3.3. Electrochemical properties

Fig. 5 shows the CVs of the TN/DNA/nano-TiO_2/GCE in 0.1 M PBS (pH 7.0) at different scan rates. One reversible redox couple was observed at $E^{0'}$ −0.19 V vs. Ag/AgCl. Also, the electrochemical responses of the TN/DNA/nano-TiO_2/GCE are anticipated for a surface-confined redox couple, because the peak currents were directly proportional to the scan rate up to 200 mV s^{-1} (Fig. 5), as predicted for a surface-confined electrochemical process [35]. The ratio of cathodic to anodic peak currents at various scan rates was almost constant. The peak-to-peak potential separation ($\Delta E_p = E_{pa} - E_{pc}$) is about 30 mV for TN redox peaks at sweep rates below 100 mV s^{-1}, suggesting facile charge transfer kinetics over this range of sweep rate. The surface coverage concentration (Γ) of TN was evaluated from the following equation:

$$\Gamma = \frac{Q}{nFA} \quad (5)$$

where A (=0.0707 cm^2) is the area of the GCE, n (=2) the number of electrons per reactant molecule, Q the charge obtained by integrating the anodic peak at low voltage scan rate (10 mV s^{-1}), and F is the Faraday constant. We assume that all of the immobilized redox centers are electroactive on the voltammetry time scale. In the present case, the calculated value of Γ was 4.5584×10^{-10} mol/cm^2. The formal potential of TN redox peak was pH-dependent (Fig. S1). A plot of $E^{0'}$ vs. pH gives a straight line from pH 1 to 7 with a slope of −62 mV/pH which is very close to the anticipated Nernstian value of −59 mV for a two-electron–two-proton process of TN [34,36] (Scheme 1) and another straight line was obtained from pH 8 to 13 with a slope of −36 mV which is due to the two-electron–one-proton electron-transfer reaction. Similar observation was reported for TN on carbon nanotube modified electrodes [34].

3.4. Electrocatalytic mediated reduction of H_2O_2

To investigate electrocatalytic activity of TN/DNA/nano-TiO_2/GCE, electrochemical catalytic reduction H_2O_2 was investigated by cyclic voltammetry (Fig. 6). There was no reduction peak observed at bare GCE and nano-TiO_2/GCE in the presence of H_2O_2 in the potential range of 0.2 to −0.7 V, suggesting that nano-TiO_2/GCE was inactive to the direct reduction of H_2O_2 (curves a'). However, at TN/DNA/nano-TiO_2/GCE, the reduction peak current at about −0.20 V was greatly enhanced in the presence of

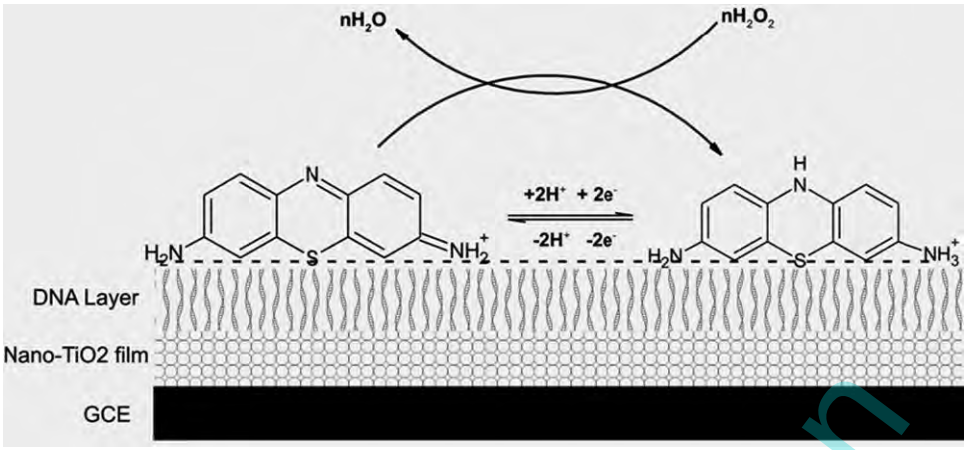

Scheme 1. Schematic representation of redox reaction of TN and electrocatalytic reduction of H_2O_2.

H_2O_2 corresponding with the decrease of the oxidation peak current, suggesting a typical excellent electrocatalytic reduction process of H_2O_2. The reduction peak current increased with the concentration of H_2O_2 in the solutions (curve b–e). In the absence of H_2O_2 a reversible redox peak of TN was retained. The above results indicated that mediated reduction of H_2O_2 takes place at TN/DNA/nano-TiO_2/GCE. According to the earlier reports [34,37] and based on our experimental findings the possible electrochemical reduction mechanism of H_2O_2 at TN modified electrode was presented in Eqs. (6) and (7).

$$\text{Thionin (oxidized form)} + 2e^- + 2H^+ \leftrightarrow \text{Thionin (reduced form)} \quad (6)$$

$$\text{Thionin (reduced form)} + H_2O_2 + 2H^+ \rightarrow \text{Thionin (oxidized form)} + 2H_2O \quad (7)$$

To ascertain the need of bi-layer films, the electrochemical depositions of TN onto bare GCE (a), nano-TiO_2/GCE (b) and DNA/nano-TiO_2/GCE (c) were carried out and the obtained results are shown in Fig. 7. From the CVs one can understand that the DNA/nano-TiO_2 nanocomposite modified electrode is highly suitable for adsorption of TN molecules. The magnitude of TN peak current on DNA/nano-TiO_2/GCE (c) was six times higher than on a bare GCE (a) and nano-TiO_2/GCE (b) which indicated the advantages of bi-layer modified electrode. After the modification, those three electrodes are washed thoroughly with pH 7 buffer solution and then CVs were recorded in pH 7.0 PBS. In contrast to TN/DNA/nano-TiO_2/GCE, redox peak currents of TN/GCE and TN/nano-TiO_2/GCE are continuously decreased and the redox peak disappeared after 20 cycles. This study clearly indicated that there is no strong dye adsorption on these electrodes which indicated the leaching of dye molecules from the electrode surface. Indirectly this study indicated that, bare GCE and nano-TiO_2 modified electrodes are not suitable for fabrication of stable amperometric sensor for the detection of H_2O_2. Nevertheless, reproducible results could not be obtained for the measurement for H_2O_2 at TN/DNA/GCE; it may due to the instability of TN/DNA film on the electrode surface.

3.5. Effect of solution pH and scan rate

The effect of pH on the response of the modified electrode was investigated in different pH solutions (1–13). This experimental result showed that the TN redox peak currents increased with the increasing pH until it reached 7.0. Thereafter, the redox peak cur-

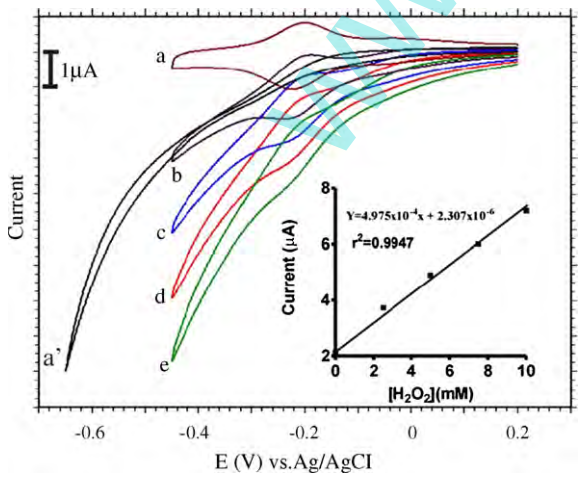

Fig. 6. Electrocatalytic reduction of H_2O_2 in pH 7.0 PBS at TN/DNA/nano-TiO_2/GCE. (a) 0.0 M, (b) 2.5×10^{-3} M, (c) 5×10^{-3} M, (d) 7.5×10^{-3} M, (e) 1×10^{-2} M H_2O_2 and (a') nano-TiO_2/GCE in 1×10^{-2} M H_2O_2.

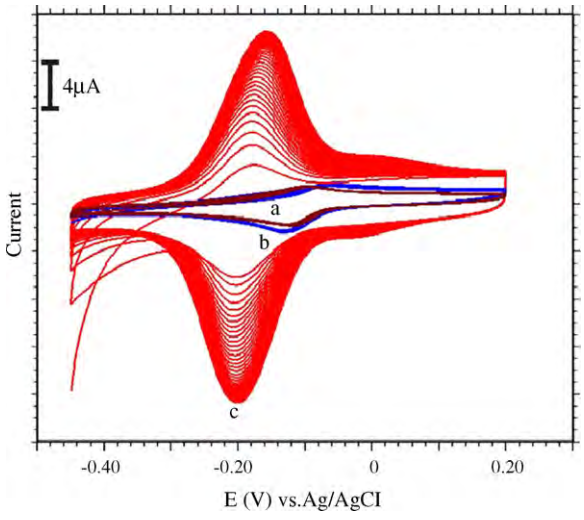

Fig. 7. CVs of TN deposition onto DNA/nano-TiO_2/GCE (c), bare GCE (b) and nano-TiO_2/GCE (a) from PBS (pH 7.0) containing 1×10^{-5} M TN.

Table 1
Comparison of the analytical data obtained by some modified electrodes proposed for the determination of H_2O_2

Electrode material	Modifier	pH	E_{pc} (V)	Linear range (M)	Detection limit (μM)	Reference
Au electrode	HRP/DNA/cysteamine	6.9	−0.20	1×10^{-5} to 9.7×10^{-3}	0.5	[18]
Au electrode	DNA–hemoglobin	5.0	−0.75	2.5×10^{-5} to 1.25×10^{-4}	0.4	[22]
Graphite electrode	Multiwalled carbon nanotubes/thionine	7.0	−0.20	1.37×10^{-6} to 3.44×10^{-4}	–	[36]
GCE	Thionin–multiwalled carbon nanotubes	7.0	−0.30	2.0×10^{-5} to 1.60×10^{-4}	0.38	[37]
GCE	Poly(*p*-aminobenzene sulfonic acid)	7.0	−0.70	5×10^{-5} to 5.5×10^{-4}	10	[38]
Screen printed carbon electrode	FAD/TiO_2	7.0	−0.45	0.15×10^{-6} to 3.0×10^{-3}	0.1	[39]
GCE	TN/DNA/nano-TiO_2	7.0	−0.2	5×10^{-5} to 2.23×10^{-2}	50	Proposed method

rents decreased with increasing pH value. Therefore, pH 7.0 PBS has been chosen as supporting electrolyte in the following experiments.

To ascertain the effect of scan rate on electrocatalytic reduction of H_2O_2 at TN/DNA/nano-TiO_2/GCE, CVs were recorded in pH 7.0 PBS containing 2.5 mM H_2O_2. The relationship between the peak current and the scan rate is shown in Fig. S2. It was found that scan rates from 10 to 200 mV s^{-1} show a linear response on the peak current at the modified electrode in the presence of H_2O_2. The result indicated that the electron-transfer reaction was controlled by surface controlled process. Based on our experimental results and according to literature report [37] electrochemical reduction mechanism of H_2O_2 at TN/DNA/nano-TiO_2/GCE is described in Scheme 1.

3.6. Amperometric determination of H_2O_2

Next, we attempted to study the amperometric measurement of H_2O_2 at TN/DNA/nano-TiO_2/GCE. The working potential was fixed at −0.2 V, the response current to the successive addition of different concentrations of H_2O_2 at the working electrode was measured (Fig. 8). The measured current was subtracted from the background current (1.2 μA) for the preparation of calibration plot. In the range of 0.05–22.3 mM, the linear regression equation was $I_p(\mu A) = 6.07e^{-4} + 1.655e^{-4}C_{H_2O_2}(\mu mol/L)$ ($r^2 = 0.9947$). The detection limit (S/N = 3) was 0.05 mM. The inset shown in Fig. 8 demonstrates the linear relationship of the electrocatalytic current (I_{cat}) vs. H_2O_2 concentration in the wide range of 0.05–22.3 mM. Analytical data of proposed method such as linear range, detection limit, applied potential and pH were compared with earlier literature reports (Table 1). From the data shown in Table 1, H_2O_2 can be determined at lower potential [22,37–39] and wide linear range of detection can be achieved using the proposed method [18,22,36–39].

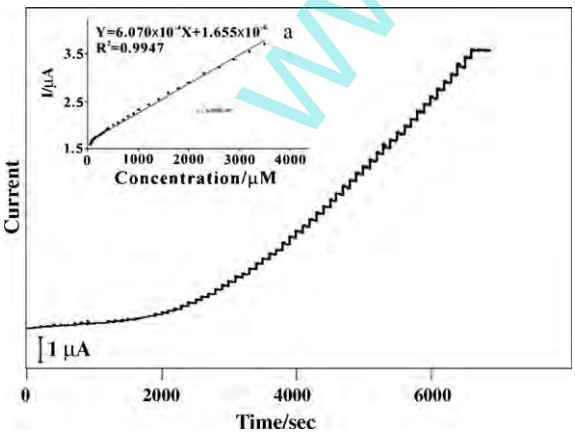

Fig. 8. Amperometric current–time curves for H_2O_2 reduction at TN/DNA/nano-TiO_2/GCE. Electrodes were held at an applied potential of −0.2 V (vs. Ag/AgCl) and rotated at 1000 rpm in a 25 mL phosphate buffer solution. Concentrations were used in the range between 0.05 and 22.3 mM H_2O_2.

3.7. Analysis of real samples

To investigate the actual applicability of the developed new biosensor TN/DNA/nano-TiO_2/GCE system to practical usage, the H_2O_2 concentrations of commercial antiseptic solutions and soft-contact lenses cleaning solutions (~3%) were analyzed. The H_2O_2 content in commercial samples has been estimated directly with the TN/DNA/nano-TiO_2/GCE by an amperometric method and the results are compared with an alternate standard method [40]. The amperometric current–time response recorded for the reduction of H_2O_2 in commercial samples for sequential additions of 10 μL of the as-prepared antiseptic agent with 200 times dilution to a 0.1 M PBS. Comparing with the linear calibration graph displayed by the TN/DNA/nano-TiO_2/GCE, an average H_2O_2 concentration was obtained over nine measurements with relative errors −1.993% and −2.276% indicating good reproducibility of the electrode (Table 2).

3.8. Reproducibility and stability of the modified electrode

The reproducibility of the current response of the biosensor was examined at fixed concentration of H_2O_2 (1.5 mM) and the relative standard deviation (RSD) was 2.3 ($n = 9$). This RSD value is better and well comparable with the existing methods [24,36–39]. It indicated that the sensor possessed good reproducibility. In addition, catalytic current response for reduction of H_2O_2 at TN/DNA/nano-TiO_2/GCE was tested in the solution containing 1.5 mM H_2O_2 before and after continuous stirring of the buffer solution for 30 min. The response of the electrode had no significant change before and after stirring the solution, this test indicated that reproducible results could be obtained at TN/DNA/nano-TiO_2/GCE. After those experiments, the biosensor was kept in 0.1 M PBS at 4 °C in order to keep the activity of TN. We used the biosensor to detect H_2O_2 three times every day and the results showed that the catalytic current decreased only about 2.0% after a month. This study indicated that TN/DNA/nano-TiO_2/GCE has good stability and it can be used repeatedly. To ascertain the reproducibility and reliability of the fabrication procedure, seven times GCE electrode was modified with TN/DNA/nano-TiO_2 films and CVs of the biosensors were recorded in 0.1 M PBS. The RSD value of measured anodic peak currents was 2.86%. The positively charged TN (pK_a 7.8) [34] monomers that were firmly attached onto negatively charged DNA/nano-TiO_2 bi-layer film may attribute to higher stability and good analytical performance of the new biosensor.

Table 2
Determination of H_2O_2 in commercial samples

Sample	H_2O_2 labeled value (%)	Proposed method % ± RSD (%)[a]	Standard method[b] (%)	Relative error (%)
1	3	2.8345 ± 1.25 ($n = 9$)	2.891	−1.993
2	3	2.7641 ± 1.84 ($n = 9$)	2.827	−2.276

[a] Relative standard deviation.
[b] Average value of three measurements.

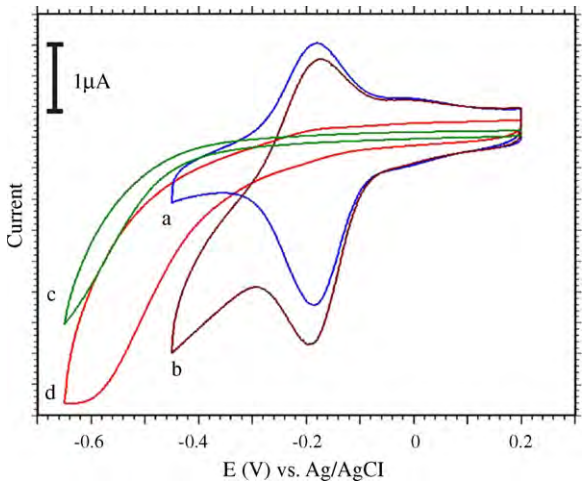

Fig. 9. Electrocatalytic reduction of O_2 in pH 7.0 PBS using TN/DNA/nano-TiO_2/GCE. (a) N_2-saturated solution, (b) O_2-saturated solution, (c) nano-TiO_2/GCE in O_2-saturated solution and (d) bare GCE in O_2-saturated solution.

3.9. Electrocatalysis of oxygen

Electrocatalytic reduction of O_2 was studied using TN/DNA/nano-TiO_2/GCE. Fig. 9 shows the CVs of TN/DNA/nano-TiO_2/GCE in 0.1 M PBS (pH 7.0) with O_2-saturated solution. An increase in the cathodic peak at about −0.20 V is observed in the presence of O_2 and the increase in the cathodic peak is accompanied by a decrease of anodic peak, suggesting that TN has mediated the electrocatalytic reduction of O_2 (curve b). Nano-TiO_2/GCE (curve c) and bare GCE (curve d) did not shown significant increase in peak current and failed to reduce the overpotential required for O_2 reduction reaction. Indeed, TN/DNA/nano-TiO_2/GCE reduced the overpotential about 430 mV. In nitrogen saturated solution a TN redox peak re-appeared (curve a). The mechanism of catalytic reduction of O_2 at TN/DNA/nano-TiO_2/GCE can be elucidated by the pathway suggested in Eq. (8). Electrochemical reduced form of TN on DNA/nano-TiO_2/GCE gets converted to oxidized form at the electrode surface followed by a fast reaction of $TN_{(red)}$ with O_2. The product of $TN_{(red)}$–O_2 could then undergo electrochemical reduction at the potential of $TN_{(oxid)}$ reduction producing H_2O_2 and $TN_{(red)}$ again [37].

$$TN_{(\text{reduced form})} + O_2 + 2H^+ \rightarrow TN_{(\text{oxidized form})} + H_2O_2 \quad (8)$$

4. Conclusions

The electrochemical preparation of nano-TiO_2 particles and their use in the preparation of amperometric biosensor for the detection of H_2O_2 was demonstrated. The TN/DNA/nano-TiO_2/GCE showed excellent stability and electrocatalytic activity towards the reduction of H_2O_2 and O_2 in physiological condition. AFM, SEM and X-ray diffraction images revealed that nano-TiO_2 particles cover the electrode surface and lead to the adsorption of DNA and TN films. The electrocatalytic properties of modified electrode were studied by using cyclic voltammetry and amperometry. The TN/DNA/nano-TiO_2/GCE has been employed as a biosensor for determination of H_2O_2 in the range from 0.05 to 22.3 mM with a detection limit of 0.05 mM (S/N = 3). We also demonstrated the real application of our proposed method for the determination of H_2O_2 in commercially available peroxide solutions with satisfactory results.

Acknowledgements

This project work was financially supported by the Ministry of Education and the National Science Council of Taiwan, ROC.

Appendix A. Supplementary data

Supplementary data associated with this article can be found, in the online version, at doi:10.1016/j.colsurfb.2008.07.003.

References

[1] X.-Q. Gong, A. Selloni, M. Batzill, U. Diebold, Steps on anatase TiO_2(1 0 1), Nat. Mater. 5 (2006) 665–670.
[2] A. Mills, S.L. Hunte, An overview of semiconductor photocatalysis, J. Photochem. Photobiol. A: Chem. 108 (1997) 1–35.
[3] M.R. Hoffmann, S.T. Martin, W. Choi, D.W. Bahnemann, Environmental application of semiconductor photocatalysis, Chem. Rev. 95 (1995) 69–96.
[4] T. Matsunaga, R. Tomoda, T. Nakajima, N. Nakamura, T. Komine, Continuous-sterilization system that uses photosemiconductor powders, Appl. Environ. Microbiol. 54 (1988) 1330–1333.
[5] Q.X. Jiai, T.M. Mccleskey, A.K. Burrell, Y. Lin, G.E. Collis, H. Wang, A.D.Q. Li, S.R. Foltyn, Polymer-assisted deposition of metal-oxide films, Nat. Mater. 3 (2004) 529–532.
[6] E. Hosono, S. Fujihara, H. Imai, I. Honma, I. Masaki, H. Zhou, One-step synthesis of nano–micro chestnut TiO_2 with rutile nanopins on the microanatase octahedron, ACS Nano 1 (2007) 273–278.
[7] T. Paunesku, T. Rajh, G. Wiederrecht, J. Maser, S. Vogt, N.A. Stojicevic, M. Protic, B. Lai, J. Oryhon, M. Thurnauer, G. Woloschak, Biology of TiO_2–oligonucleotide nanocomposites, Nat. Mater. 2 (2003) 343–346.
[8] W.C.-W. Chan, S.M. Nie, Quantum dot bioconjugates for ultrasensitive nonisotopic detection, Science 281 (1998) 2016–2018.
[9] T.A. Taton, C.A. Mirkin, R.L. Letsinger, Scanometric, DNA array detection with nanoparticle probes, Science 289 (2000) 1757–1760.
[10] S.-J. Park, T.A. Taton, C.A. Mirkin, Array-based electrical detection of DNA with nanoparticle probes, Science 295 (2002) 1503–1506.
[11] Y. Wei, C. Cao, R. Jin, C.A. Mirkin, Nanoparticles with Raman spectroscopic fingerprints for DNA and RNA detection, Science 297 (2002) 1536–1540.
[12] C. Ogino, K. Kanehira, R. Sasai, S. Sonezaki, N. Shimizu, Recognition and effective degradation of 17β-estradiol by anti-estradiol-antibody-immobilized TiO_2 nanoparticles, J. Biosci. Bioeng. 104 (2007) 339–342.
[13] S.K. Lunsford, H. Choi, J. Stinson, A. Yeary, D.D. Dionysiou, Voltammetric determination of catechol using a sonogel carbon electrode modified with nanostructured titanium dioxide, Talanta 73 (2007) 172–177.
[14] S. Yuan, S. Hu, Characterization and electrochemical studies of Nafion/nano-TiO_2 film modified electrodes, Electrochim. Acta 49 (2004) 4287–4293.
[15] H. Zhou, X. Gan, T. Liu, Q. Yang, G. Li, Electrochemical study of photovoltaic effect of nano titanium dioxide on hemoglobin, Bioelectrochemistry 69 (2006) 34–40.
[16] H. Zhou, X. Gan, J. Wang, X. Zhu, G. Li, Hemoglobin-based hydrogen peroxide biosensor tuned by the photovoltaic effect of nano titanium dioxide, Anal. Chem. 77 (2005) 6102–6104.
[17] B. Filanovsky, B. Markovsky, T. Bourenko, N. Perkas, R. Persky, A. Gedanken, D. Aurbach, Carbon electrodes modified with TiO_2/metal nanoparticles and their application to the detection of trinitrotoluene, Adv. Funct. Mater. 17 (2007) 1487–1492.
[18] Y.H. Song, L. Wang, C.B. Ren, G.Y. Zhu, Z. Li, A novel hydrogen peroxide sensor based on horseradish peroxidase immobilized in DNA films on a gold electrode, Sens. Actuators B: Chem. 114 (2006) 1001–1006.
[19] X.H. Chen, C.M. Ruan, J.L. Kong, J.Q. Deng, Characterization of the direct electron transfer and bioelectrocatalysis of horseradish peroxidase in DNA film at pyrolytic graphite electrode, Anal. Chim. Acta 412 (2000) 89–98.
[20] C. Fan, G. Li, J. Zhu, D. Zhu, A reagentless nitric oxide biosensor based on hemoglobin–DNA films, Anal. Chim. Acta 423 (2000) 95–100.
[21] H.H. Landin, D. Segerback, C. Damberg, S.O. Golkar, Adducts with haemoglobin and with DNA in epichlorohydrin-exposed rats, Chem. Biol. Interact. 117 (1999) 49–64.
[22] A.K.M. Kafi, F. Yin, H.K. Shin, Y.S. Kwon, Hydrogen peroxide biosensor based on DNA–Hb modified gold electrode, Thin Solid Films 499 (2006) 420–424.
[23] A.E.F. Nassar, J.F. Rusling, Electron transfer between electrodes and heme proteins in protein-DNA films, J. Am. Chem. Soc. 118 (1996) 3043–3044.
[24] Z. Tong, R. Yuan, Y. Chai, S. Chen, Y. Xie, Amperometric biosensor for hydrogen peroxide based on hemoglobin/DNA/poly-2,6-pyridinediamine modified gold electrode, Thin Solid Films 515 (2007) 8054–8058.
[25] X. Lin, G. Kang, L. Lu, DNA/Poly(*p*-aminobenzensulfonic acid) composite bilayer modified glassy carbon electrode for determination of dopamine and uric acid under coexistence of ascorbic acid, Bioelectrochemistry 70 (2007) 235–244.
[26] X. Li, Y. Chen, X. Huang, Electrochemical behavior of neomycin at DNA-modified gold electrodes, J. Inorg. Biochem. 101 (2007) 918–924.

[27] X.H. Jiang, X.Q. Lin, Atomic force microscopy of DNA self-assembled on a highly oriented pyrolytic graphite electrode surface, Electrochem. Commun. 6 (2004) 873–879.
[28] X.Q. Lin, X.H. Jiang, L.P. Lu, DNA nano-netting intertexture on carbon electrodes, Chin. Chem. Lett. 5 (2004) 997–1000.
[29] X.Q. Lin, X.H. Jiang, L.P. Lu, DNA deposition on carbon electrodes under controlled DC potentials, Biosens. Bioelectron. 20 (2005) 1709–1717.
[30] J. Georgieva, S. Armyanov, E. Valova, I. Poulios, S. Sotiropoulos, Preparation and photoelectrochemical characterisation of electrosynthesised titanium dioxide deposits on stainless steel substrates, Electrochim. Acta 51 (2006)2076–2087.
[31] S. Karuppuchamy, D.P. Amalnerkar, K. Yamaguchi, T. Yoshida, T. Sugiura, H. Minoura, Cathodic electrodeposition of TiO_2 thin films for dye-sensitized photoelectrochemical applications, Chem. Lett. 143 (2001)78–79.
[32] S. Karuppuchamy, K. Nonomura, T. Yoshida, T. Sugiura, H. Minoura, Cathodic electrodeposition of oxide semiconductor thin films and their application to dye-sensitized solar cells, Solid State Ion 151 (2002) 19–27.
[33] L.P. Lu, X.Q. Lin, Glassy carbon electrode modified with gold nanoparticles and DNA for the simultaneous determination of uric acid and norepinephrine under coexistence of ascorbic acid, Anal. Sci. 20 (2004) 527–530.
[34] A. Salimi, A. Noorbakhsh, S. Soltanianb, Electroless deposition of thionin onto glassy carbon electrode modified with single wall and multiwall carbon nanotubes: improvement of the electrochemical reversibility and stability, Electroanalysis 18 (2006) 703–711.
[35] A.J. Bard, L.R. Faulkner, Electrochemical Methods Fundamentals and Applications, Wiley, New York, 1980, pp. 521–525.
[36] D.R. Shobha Jeykumari, S. Ramaprabhu, S. Sriman Narayanan, A thionine functionalized multiwalled carbon nanotube modified electrode for the determination of hydrogen peroxide, Carbon 45 (2007) 1340–1353.
[37] A. Salimi, A. Noorbakhsh, H. Mamkhezri, R. Ghavamia, Electrocatalytic reduction of H_2O_2 and oxygen on the surface of thionin incorporated onto MWCNTs modified glassy carbon electrode: application to glucose detection, Electroanalysis 19 (2007) 1100–1108.
[38] S.A. Kumar, S.-M. Chen, Electrocatalytic reduction of oxygen and hydrogen peroxide at poly(*p*-aminobenzene sulfonic acid)-modified glassy carbon electrodes, J. Mol. Catal. A: Chem. 278 (2007) 244–250.
[39] S.A. Kumar, P.-H. Lo, S.-M. Chen, Electrochemical synthesis and characterization of TiO_2 nanoparticles and their use as a platform for flavin adenine dinucleotide immobilization and efficient electrocatalysis, Nanotechnology 19 (2008) 255501.
[40] E. Graf, J.T. Penniston, Method for determination of hydrogen peroxide, with its application illustrated by glucose assay, Clin. Chem. 26 (1980) 658–660.